Journal Pre-proofs

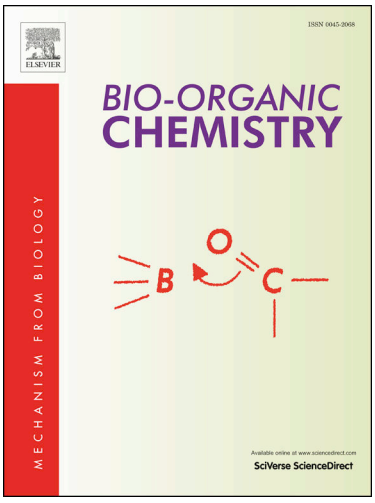

Pyridoxine-resveratrol hybrids as novel inhibitors of MAO-B with antioxidant and neuroprotective activities for the treatment of Parkinson's disease

Wei Li, Xia Yang, Qing Song, Zhongcheng Cao, Yichun Shi, Yong Deng, Li Zhang

PII: S0045-2068(19)32220-5
DOI: https://doi.org/10.1016/j.bioorg.2020.103707
Reference: YBIOO 103707

To appear in: *Bioorganic Chemistry*

Received Date: 25 December 2019
Revised Date: 14 February 2020
Accepted Date: 26 February 2020

Please cite this article as: W. Li, X. Yang, Q. Song, Z. Cao, Y. Shi, Y. Deng, L. Zhang, Pyridoxine-resveratrol hybrids as novel inhibitors of MAO-B with antioxidant and neuroprotective activities for the treatment of Parkinson's disease, *Bioorganic Chemistry* (2020), doi: https://doi.org/10.1016/j.bioorg.2020.103707

Pyridoxine-resveratrol hybrids as novel inhibitors of MAO-B with antioxidant and neuroprotective activities for the treatment of Parkinson's disease

Wei Li[a,1], Xia Yang[a,1], Qing Song[a], Zhongcheng Cao[a], Yichun Shi[a], Yong Deng[a,*], Li Zhang[b,*]

[a]*Department of Medicinal Chemistry, Key Laboratory of Drug-Targeting and Drug Delivery System of the Education Ministry and Sichuan Province, Sichuan Engineering Laboratory for Plant-Sourced Drug and Sichuan Research Center for Drug Precision Industrial Technology, West China School of Pharmacy, Sichuan University, Chengdu 611041, China*

[b]*Department of Elderly Digestive, Sichuan Academy of Medical Sciences & Sichuan Provincial People's Hospital, Chengdu,610072, China*

[1] These authors contributed equally to this work.

**Corresponding Author*.

E-mail: dengyong@scu.edu.cn (Yong Deng), ZL.gLx.gjq@163.com (Li Zhang)

Abstract

A series of pyridoxine-resveratrol hybrids were designed and synthesized as monoamine oxidase B inhibitors for the treatment of Parkinson's disease. Most of them exhibited potent inhibitory activities on MAO-B with high selectivity. Specifically, compounds **12a**, **12g** and **12l** showed the most excellent inhibition to *h*MAO-B with the IC_{50} values of 0.01 μM, 0.01 μM and 0.02 μM, respectively. Further reversibility study demonstrated that **12a** and **12l** were reversible and **12g** was irreversible MAO-B inhibitors. Molecular docking studies of MAO revealed the binding mode and high selectivity of these compounds with MAO-B. In addition, these three representative compounds also exhibited low cytotoxicity and excellent neuroprotective effect in the test on H_2O_2-induced PC-12 cell injury. Moreover, **12a**, **12g** and **12l** showed good antioxidant activities and high blood-brain barrier permeability. Overall, all of these results highlighted **12a**, **12g** and **12l** were potential and excellent MAO-B inhibitors for PD treatment.

Keywords:

Parkinson's disease; Pyridoxine-resveratrol hybrids; MAO-B inhibitors; Reversibility; Antioxidant; Neuroprotective agents.

1. Introduction

Parkinson's disease (PD) is the world's second common age-associated and progressive neurodegenerative disease. It is characterized by motor behavioral abnormalities (resting tremors, bradykinesia, postural instability and rigidity), and accompanied the non-motor symptoms consisting neuropsychiatric symptoms (depression, cognitive dysfunctions and dementia), sleep disturbance (insomnia, rapid eye movement disorders, vivid dreaming), autonomic symptoms (bladder disorders, orthostatic hypotension) and anosmia [1-3]. With the increase of average life expectancy, PD has become a severe social and economic problem. About 0.3% of the general population and 1-3% of the population over the age of 65 are affected by PD. Unfortunately, the number of people who suffer from PD is going to rise from 8.7 to 9.3 million by 2030 [4, 5]. The main pathologies of PD include the progressive degeneration of dopaminergic neurons in the substantia nigra pars compacta of the midbrain, the presence of lewy bodies mainly formed by fibrillar α-synuclein and the mitochondrial dysfunction in CNS [6-8]. Recent reports indicated that oxidative stress and inflammation also participate in the disease pathogenesis [9-11].

Monoamine oxidase B (MAO-B) with flavin adenine dinucleotide (FAD) as the cofactor, is present in the outer mitochondrial membrane [12]. It is mainly utilized to catalyze the oxidative deamination (e.g., dopamine, tyramine, benzylamine, phenylethamine), which participates in Fenton-type reactions with Fe (II) to generate reactive oxygen species [12]. Some evidence suggests that MAO-B activity increases in the human brain with age, and elderly PD patients have been proved to show a high MAO-B catalytic rate in their brain. This probably reduces the central dopamine (DA) supply and increases the production of hydrogen peroxide and aldehyde species, which may cause the neurodegeneration associated with PD [12, 13]. So drugs with inhibition of MAO-B are necessary in PD therapy.

It is widely believed that the pathology of PD are associated with oxidative stress [1, 9, 11]. Oxidative stress mainly comes from the overproduction of reactive oxygen species (ROS) such as hydroxyl radical (OH) and lipid peroxide radical (ROO^-) [14]. In human body, many enzymatic reactions and metabolic events have been considered as the major endogenous sources of ROS [9]. When ROS productions surpass the antioxidant capacity of a cell, it will lead to oxidative stress, cause irreversible damage to cellular macromolecules and can ultimately result in cell death [12]. Therefore, protection of neuronal cells from oxidative stress is a potential therapeutic strategy for the

treatment of PD.

The existing therapies for PD include dopamine pathway, anticholinergics and deep brain stimulation. All currently approved therapies to increase striatal dopamine levels include levodopa, dopamine agonists, MAO-B inhibitors (such as rasagiline, selegiline, safinamide and so on), catechol-*O*-methyltransferase inhibitors and amantadine [15-17]. Unfortunately, these therapies do not represent a long-term solution, and there is no disease-modify treatment for PD [6]. In order to achieve better therapeutic effect, multiple medication therapies and multiple compound medications both have been applied. However, the hidden drawbacks include complex ADMET properties and possible drug-drug interactions leading to severe side effects. A multifunctional compound that can exert multiple bioactivities may be an optimum choice [18, 19].

Resvertrol (RSV) is a polyphenol presented in a variety of plants, such as grapes, peanuts, berries and so on. In recent years, RSV has been revealed to possess a variety of beneficial properties which include anti-oxidant, anti-inflammatory, anti-apoptosis, anti-steatotic, anti-proliferative and neuroprotective properties [20-23]. Some studies also showed that RSV derivatives had a character of MAO-B inhibition [24]. Pyridoxine (vitamin B_6) is considered to be an enzymatic cofactor for at least 140 enzymes [25]. In addition to its regulatory role, pyridoxine has also been shown to be an antioxidant. It can inhibit the production of radicals and serve as quenchers for single oxygen [26, 27]. Because of their versatile properties which are beneficial for the treatment of neurodegenerative diseases, in our previous works, we designed and synthesized a series of pyridoxine-resvertrol hybrids Mannich base derivatives and found the intermediate bearing ketal-protected six-membered ring demonstrated excellent MAO-B inhibitory activity. According to the docking results, the isopropylidene group on the pyridine ring of the intermediate occupies the inlet cavity of the monoamine oxidase and stably binds with a series of amino acid residues through hydrophobic interaction [28]. Therefore, we suspect that the ketal-protected six-membered ring on the pyridine moiety is essential for its MAO-B inhibitory activity. In addition, these hybrids Mannich bases also showed good antioxidant activity due to the presence of one or more free hydroxyl groups [28]. However, this also brings two disadvantages: first, the presence of hydroxyl group increases the polarity of the compounds, making them low liposolubility and not good for passing the blood-brain barrier; second, the compounds are easily metabolized and excreted in the body. Therefore, in this paper, we reduced the number of free hydroxyl groups by retaining the ketal-protected six-membered

ring on the pyridine moiety and introducing different substituent on the benzene ring in order to improve their lipophilicity and the permeability of the blood-brain barrier, so that it can exert MAO-B inhibition in the central nervous system and provide a new study direction for the treatment of PD. Through the above considerations, a new series of pyridoxine-resvertrol hybrid derivatives were designed, synthesized and evaluated for their biological activities including inhibition of MAOs, reversibility study of *h*MAO-B inhibition, molecular docking studies, anti-oxidative activities, neuroprotective activity and the ability to cross the blood-brain barrier. The design strategy for pyridoxine-resveratrol hybrid derivatives is depicted in **Fig. 1**.

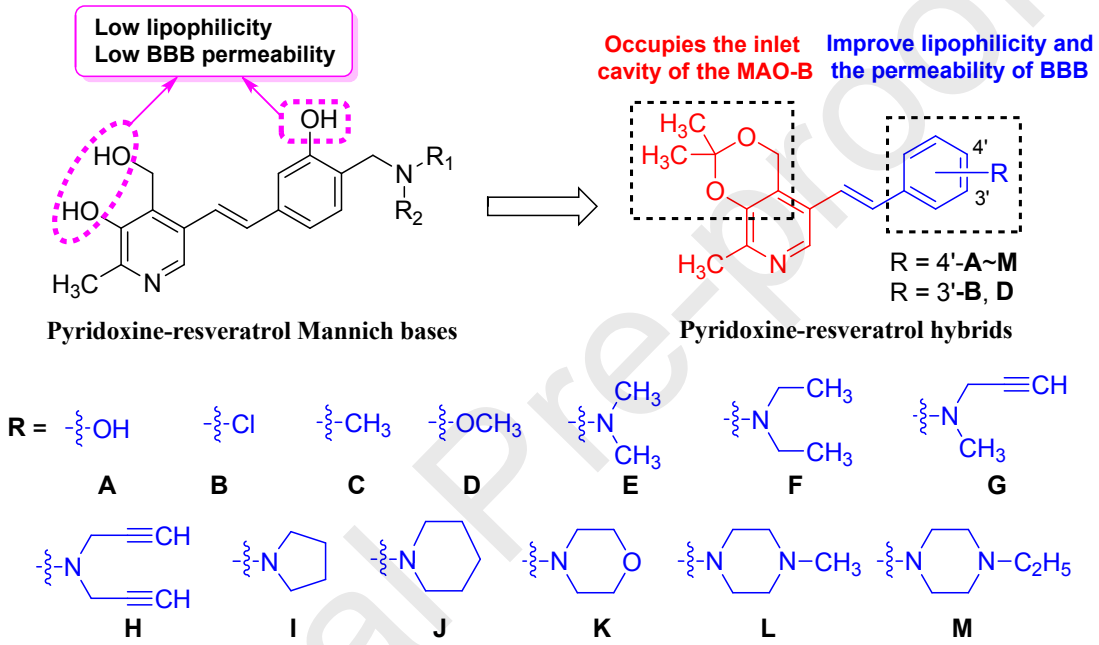

Figure 1. Design strategy for the pyridoxine-resveratrol hybrid derivatives.

2. Results and discussion

2.1. Chemistry

The synthetic pathways toward the target compounds were summarized in **Scheme 1** and **Scheme 2**. The 4-(methoxymethoxy)benzaldehydethe (**2**) was synthesized by using *p*-hydroxybenzaldehyde (**1**) as starting material, and the *para*-substituted benzaldehyde **2-1g** was prepared from aniline (**3**), through *N*-propargylation, *N*-methylation and Vilsmeier formylation reaction with DMF/$POCl_3$ [29]. For the preparation of **2-1h**, compound **3** underwent *N*-dipropargylation reaction to afford dipropargyl-substituted aniline (**6**), and then formylation by Vilsmeier reaction. The other *para*-substituted benzaldehydes **2-1i~m** were obtained by the reaction

of 4-fluorobenzaldehyde (**7**) with corresponding secondary amine [30].

The designed compounds were obtained by using the pyridoxine as starting material. In the first step, commercially available pyridoxine hydrochloride (**8**) was isopropylidene protected at the 3- and 4-hydroxy groups based on published procedures [31]. Chlorination of the hydroxymethyl on the 5-position gave intermediate **10**. **10** reacted with triethyl phosphite through Arbuzov reaction to give compound **11**, which was then subjected to a Wittig-Horner reaction with *meta*- or *para*-substituted benzaldehyde to yield target compounds **12b**-**12m** and **13a**-**13b**. However, **12a** was prepared through different synthetic route. Firstly, **11** reacted with 4-(methoxymethoxy)benzaldehyde (**2**) to obtain **14**, and then subjected to hydrolysis reaction to afford **15**. Finally, the target compound **12a** was obtained through isopropylidene protection reaction of **15**. All target compounds were not reported previously and characterized by ^{1}H NMR, ^{13}C NMR and MS.

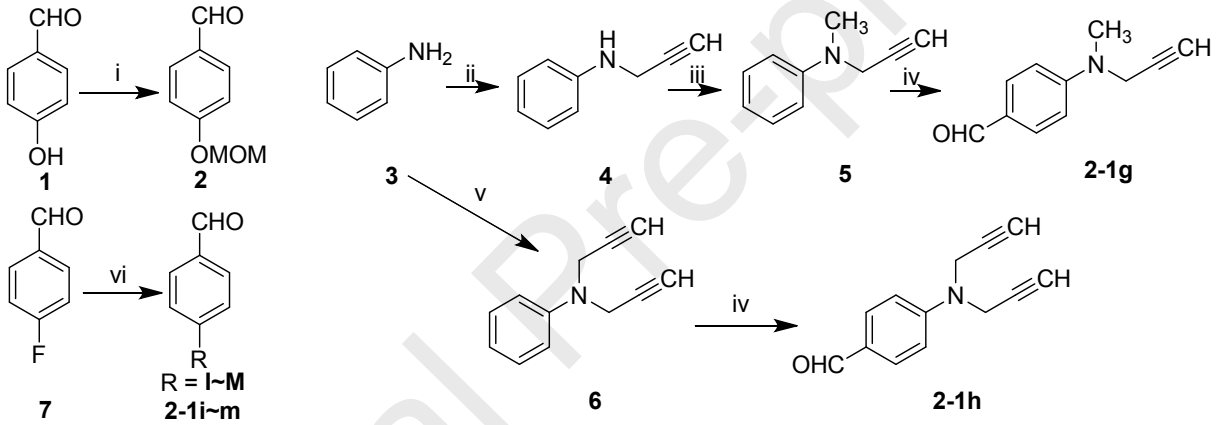

Scheme 1. Synthesis of *para*-substituted benzaldehydes (**2**, **2-1g-m**). *Reagents and conditions*: (i) *p*-hydroxybenzaldehyde, chlormethyl methyl ether, K_2CO_3, acetone, reflux for 4 h; (ii) 1.5 *eq.* propargyl bromide, K_2CO_3, DMF, at r.t. for 5 h; (iii) $(CH_3)_2SO_4$, K_2CO_3, acetone, reflux for 4 h; (iv) $POCl_3$, DMF, at 30 ^{o}C for 3 h; (v) 2.5 *eq.* propargyl bromide, K_2CO_3, DMF, at r.t. for 5 h; (vi) secondary amine, K_2CO_3, DMF, at 100 ^{o}C for 4 -6 h.

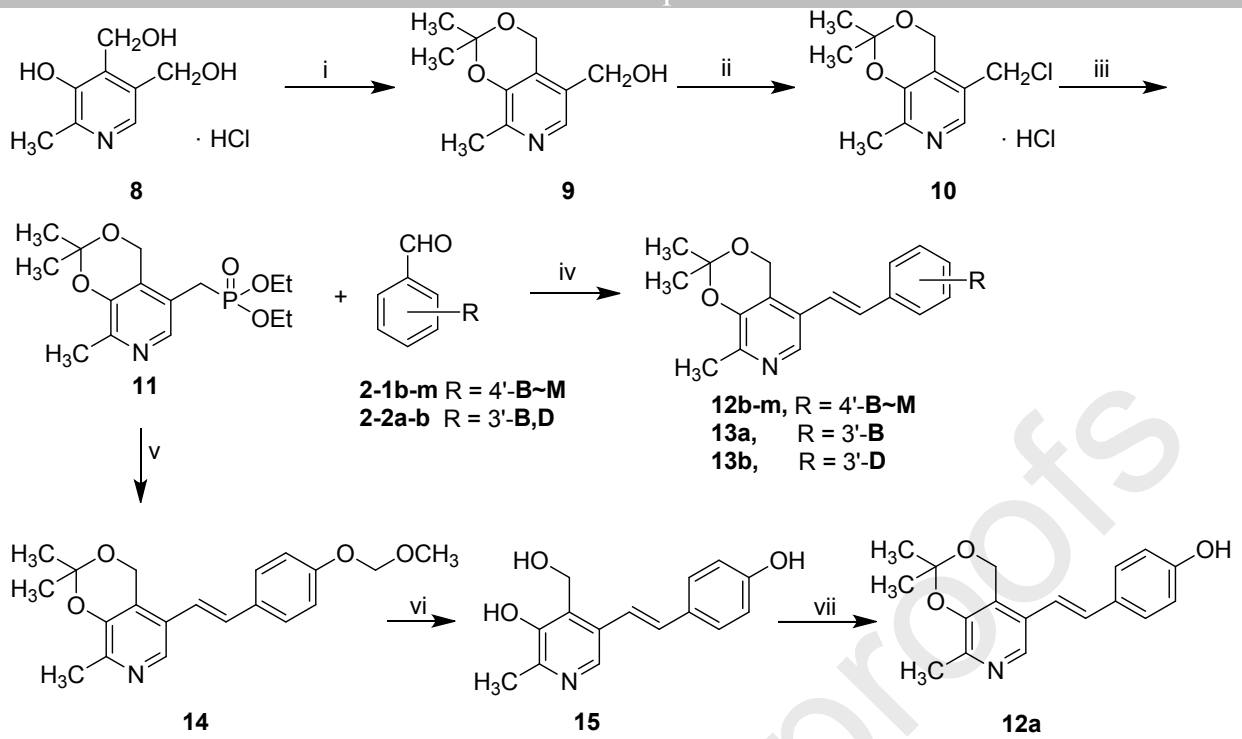

Scheme 2. Synthesis of pyridoxine-resveratrol hybrids. *Reagents and conditions*: (i) *conc.* H_2SO_4, acetone, at r.t. for overnight; (ii) $SOCl_2$, toluene, reflux for 30 min; (iii) $P(OEt)_3$, reflux for 4 h; (iv) *para*- or *meta*-substituted benzaldehydes (**2-1b~m**, **2-2a~b**), NaH, dry THF, at 0 °C for 4-7 h; (v) 4-(methoxymethoxy)benzaldehyde, NaH, dry THF, at 0 °C for 5 h; (vi) 10% HCl, THF, at 70 °C for 3 h; (vii) *conc.* H_2SO_4, acetone, at r.t. for 2 h.

2.2. Pharmacology

2.2.1. Recombinant human MAO-A and MAO -B inhibition studies

All of the synthesized compounds were evaluated for their inhibitory activities against recombinant human MAO-A and MAO-B, and use clorgyline, rasagiline and iproniazid as reference compounds. The corresponding IC_{50} values were shown in **Table 1**.

The screening results of the target compounds demonstrated that all tested compounds showed weak MAO-A inhibitory activities (percent inhibition < 45% at 10 μM). However, most compounds exhibited significant MAO-B inhibitory activities with IC_{50} values ranging from 35.87 μM to 0.01 μM. The results revealed that all pyridoxine-resveratrol hybrids were selective MAO-B inhibitors. A plenty of evidences showed that selective inhibition of MAO-B was beneficial for the treatment of PD because the inhibition of MAO-A might cause adverse effects (*e.g.* cheese reaction) [32, 33]. Among these compounds, **12a**, **12g** and **12l** had excellent MAO-B inhibitory activities with the IC_{50}

value of 0.01 μM, 0.01 μM and 0.02 μM, respectively, which were more effective than that of the positive control drugs rasagiline (IC_{50} = 0.0437 μM) and iproniazid (IC_{50} = 4.32 μM). In summary, **12a**, **12g** and **12l** were excellent MAO-B inhibitors.

Compared the MAO-B inhibitory activities of the target compounds (**12d**, **13b**), we found that compounds (**12d)** containing *para*-position substituent group performed better in inhibiting MAO-B than the one possessing *meta*-position substituent group (**13b**). The result revealed that the introduction of different substituents on *para*-position might be more helpful for improving MAO-B inhibitory activities. In addition, the assay results of the compound **12a** and **12d** showed that MAO-B inhibitory activities were significantly decreased after the hydroxyl group was methylated. It revealed that decreasing the electron-donating ability of substituent group would reduce MAO-B inhibitory activities. And compared the MAO-B inhibitory activities of the target compounds **12g** and **12h**, when the substituent group was changed from *N*-methyl-*N*-propargylamine to *N*,*N*-dipropargylamine, the MAO-B inhibitory activities was greatly reduced. The result showed that introducing another propargyl would lead to a dramatic decrease in MAO-B inhibition. In addition, compared the compounds **12e** and **12f**, we found that extending the carbon chain was not beneficial for inhibiting the activities of MAO-B. Also, we found that compound (**12i**) with cyclic amine group showed better MAO-B inhibitory activities than **12f** which was substituted by chain amine group. It reflected that compounds with cyclic amine groups might have better potential on MAO-B inhibition than compounds with chain amine groups.

Table 1 The structures of compound **12a-m**, **13a-b** and *in vitro* inhibition of MAO and oxygen radical absorbance capacity (ORAC, Trolox equivalents) by pyridoxine-resveratrol hybrids and reference compounds.

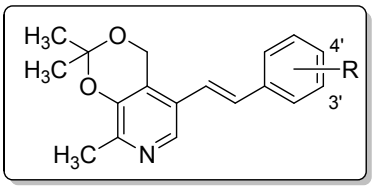

Comp.	R position	R	MAO-A inhibition(%) [a]	MAO-B IC_{50} (μM) [b]	ORAC [c]
12a	4′	-OH	24.1 ± 1.38	0.01 ± 0.003	2.89 ± 0.12
12b	4′	-Cl	n.a.[d]	n.a.[d]	N.T.[e]
12c	4′	$-CH_3$	n.a.[d]	11.35 ± 0.13	N.T.[e]

12d	4′		21.3 ± 0.58	35.87 ± 0.33	N.T.[e]
12e	4′		18.3 ± 0.12	0.68 ± 0.02	2.87 ± 0.08
12f	4′	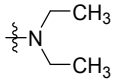	8.0 ± 0.43	27.29 ± 1.70	1.98 ± 0.15
12g	4′	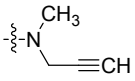	28.0 ± 3.17	0.01 ± 0.005	2.53 ± 0.07
12h	4′	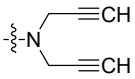	14.7 ± 1.02	10.98 ± 0.28	N.T.[e]
12i	4′		43.2 ± 1.21	0.65 ± 0.02	2.26 ± 0.12
12j	4′		10.5 ± 0.64	17.83 ± 1.88	N.T.[e]
12k	4′	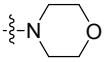	21.9 ± 0.91	1.62 ± 0.07	2.30 ± 0.10
12l	4′	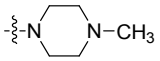	12.0 ± 0.22	0.02 ± 0.005	2.43 ± 0.09
12m	4′	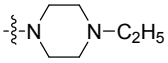	11.4 ± 0.18	23.40 ± 1.02	N.T.[e]
13a	3′		n.a.[d]	n.a.[d]	N.T.[e]
13b	3′		n.a.[d]	n.a.[d]	N.T.[e]
Clorgiline	—	—	0.0079 ± 0.0002 μM[f]	8.85 ± 0.201	N.T.[e]
Rasagiline	—	—	0.712 ± 0.021 μM[f]	0.0437 ± 0.002	N.T.[e]
Iproniazid	—	—	1.37 ± 0.043 μM[f]	4.32 ± 0.174	N.T.[e]

[a] Percentages are the percent inhibition of MAO by tested compounds at 10 μM. Data were expressed as mean ± SD.

[b] IC_{50} values represent the concentration of inhibitor required to decrease enzyme activity by 50% and are the mean of 3 independent experiments, each performed in triplicate. Data were expressed as mean ± SD.

[c] The mean ± SD of the 3 independent experiments. Data are expressed as μM of Trolox equivalent/μM of tested compound.

[d] n.a. = no active. Compounds defined "no active" means a percent inhibition of less than 5.0% at a concentration of 10 μM under the assay conditions.

[e] N.T. = not tested.

[f] IC_{50} values of the compounds

2.2.2. Reversibility study of hMAO-B inhibition

In order to further understand the binding mode of the target compounds with MAO-B, the reversibility of MAO-B inhibition by **12a**, **12g** and **12l** was investigated by measuring the recovery of MAO-B activities after dialysis of enzyme-inhibitor mixtures [34]. **12a**, **12g** and **12l** at a concentration of 4 × IC_{50} were preincubated with MAO-B for a period of 30 min and subsequently the mixtures were dialyzed for 24 h respectively. As negative and positive controls, MAO-B was also

preincubated in the absence of inhibitor, presence of a concentration equal to 4 × IC_{50} of the irreversible inhibitor rasagiline (MAO-B IC_{50} = 0.014 μM) and reversible inhibitor safinamide (MAO-B IC_{50} = 0.039 μM). For comparison, undialyzed mixtures of MAO-B-**12a**, MAO-B-**12g**, MAO-B-**12l**, MAO-B-rasagiline and MAO-B-safinamide were treated under the same conditions. The results were shown in **Fig. 2**, the catalytic activities of MAO-B inhibited by rasagiline and safinamide was restored to 5.6% and 88.5% of the control value (recorded in the absence of inhibitor) after 24 h dialysis. In contrast, the MAO-B activities in undialyzed mixtures were 1.7% and 37.2% of the control value. The results suggested that the dialysis model which was used to study the reversibility of *h*MAO-B inhibition was successful. The catalytic activity of MAO-B inhibited by the three target compounds was restored to 90.6%, 3.2% and 90.1% after 24 h dialysis. Meanwhile, the MAO-B activities in undialyzed mixtures were 36.8%, 1.5% and 38.1%. These data showed that **12a** and **12l** were reversible inhibitors, while **12g** interacted with MAO-B irreversibly. And the results were indicated that the different binding modes of these representative compounds might come from their different chemical structures. The chemical structure of **12g** was similar to rasagiline and both of them all contained the propargylamine group. There has been reported that rasagiline and its analogue *R*-M4CPAI occupied the active site cavity of MAO-B and reacted with the flavin forming an irreversible covalent adduct with the N_5 atom of the cofactor (**Fig. 3**) [35]. Therefore, the irreversible inhibitor **12g** may have the similar binding mode of rasagiline with MAO-B.

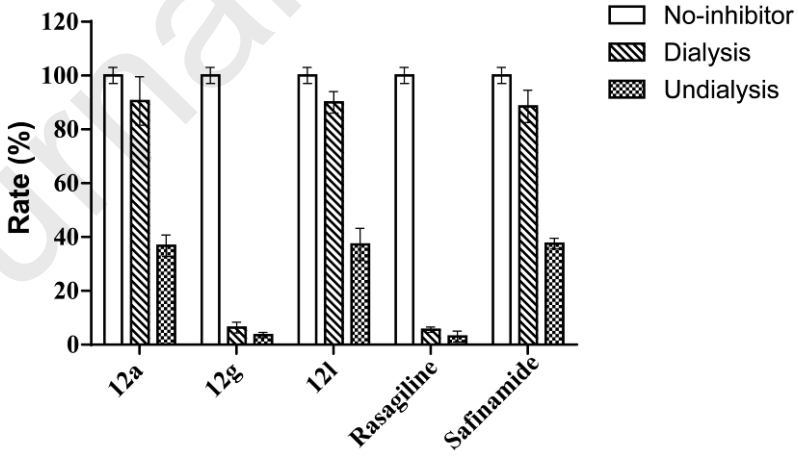

Figure 2 Reversibility of the inhibition of MAO-B by **12a**, **12g** and **12l**. MAO-B and **12a**, **12g**, **12l**, rasagiline, safinamide (at 4 × IC_{50}) were preincubated for 30 min, dialyzed for 24 h and the residual enzyme activities was measured (**12a**, **12g**, **12l**-dialysis). MAO-B was similarly preincubated in the absence (no-inhibitor) and presence of the irreversible inhibitor rasagiline (rasagiline-dialysis), reversible inhibitor safinamide (safinamide-dialysis) and dialyzed. For comparison, the residual

MAO-B activities of undialyzed mixtures of MAO-B with **12a**, **12g**, **12l**, rasagiline and safinamide was also shown. The values are given as mean ± standard deviation (SD) of triplicate determinations.

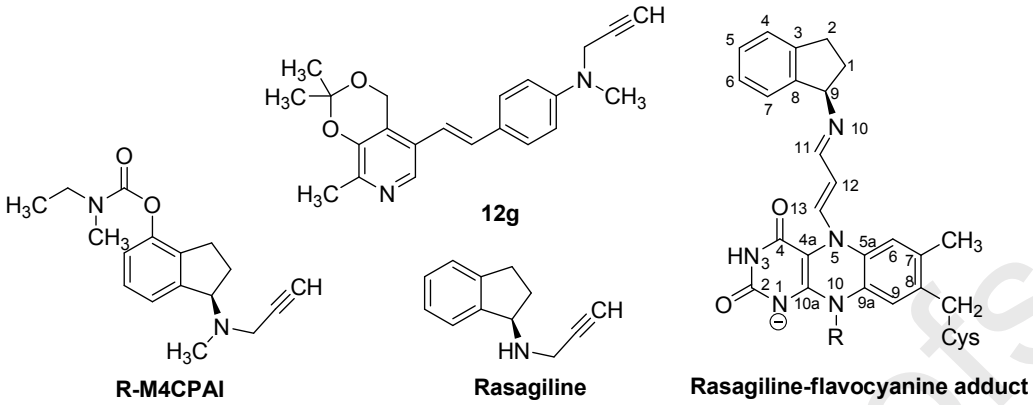

Figure 3 Chemical formula of rasagiline-related inhibitors. Irreversible inhibitors: *R*-M4CPAI, rasagiline, **12g** and rasagiline that form a covalent adduct with the flavin.

2.2.3. Molecular modeling study of MAO

To explore the possible interacting mode of the pyridoxine-resveratrol hybrids with MAOs, molecular modeling study was performed with respect to both isoforms of human MAOs. In view of the above results, we selected the most potent compound **12a** to dock with MAOs based on the X-ray crystal structures of human MAO-A (PDB code: *2Z5X*) and MAO-B (PDB code: *2V60*) [36]. To further elucidate why **12g** and **12l** displayed the similar inhibitory activities and selectivities of MAO-B as **12a**, docking studies of **12g** and **12l** with MAOs were also performed (Supplementary Material **Figure S1**). Molecular modeling study was performed using the docking program, AutoDock 4.2 package. The docking results of **12a** were shown in **Fig. 4** and the estimated binding energies of compounds **12a**, **12g** and **12l** with MAOs were shown in **Table 2**.

As shown in **Fig. 4A**, a hydrogen bond was formed between the hydroxyl group on the benzene ring of compound **12a** with Ala121. The compound **12a**-MAO-A complex was stabilized by hydrophobic interactions with Asn181, Cys323, Ile180, Ile207, Ile325, Ile335, Leu97, Phe108, Phe208, Phe352, Yyr69, Tyr407, Tyr444, Val210. As can be seen from **Fig. 4B**, the sterically hindered isopropylidene group in the pyridine ring occupied the inlet cavity of MAO-B and interacted with a series of hydrophobic residues to stabilize the complex structure of the docking compounds with MAO-B, such as Gln206, Ile199, Leu171, Pro102, Pro104, Tyr534, and so on. The benzene ring moiety of compound **12a** and MAO-B formed a complex by the π-π stacking effect with Tyr398. In addition, a hydrogen bond was observed between the hydroxyl group and Tyr 435.

Besides, the nitrogen atom on the pyridine ring formed a hydrogen bond with Tyr326. The binding energies of target compound **12a** with MAO-A and MAO-B were -9.44 kcal/mol and -11.65kcal/mol.

From the **Table 2**, we can see the reversible MAO-B inhibitors **12a** and **12g** showed similar low MAO-B binding energies but high MAO-A binding energies, which reasonably explained their excellent and selective MAO-B inhibitory activities. However, just one hydrogen bond was observed in **12g**-MAO-B complex (**Figure S1)**, while there were two in **12a**-MAO-B complex. Therefore, **12a** exhibited stronger interaction with **MAO-B** than **12g**, which gave the reason why the MAO-B inhibitory activity of **12a** was greater than that of **12g**. As for the irreversible MAO-B inhibitor **12l**, its *N*-methyl-*N*-propargylamine moiety is closed to the enzymatic cofactor FAD, indicating this moiety may form covalent bond subsequently [35]. Overall, the docking results generally showed the binding modes of pyridoxine-resveratrol hybrids, and explained the reason of their good and selective MAO-B inhibition.

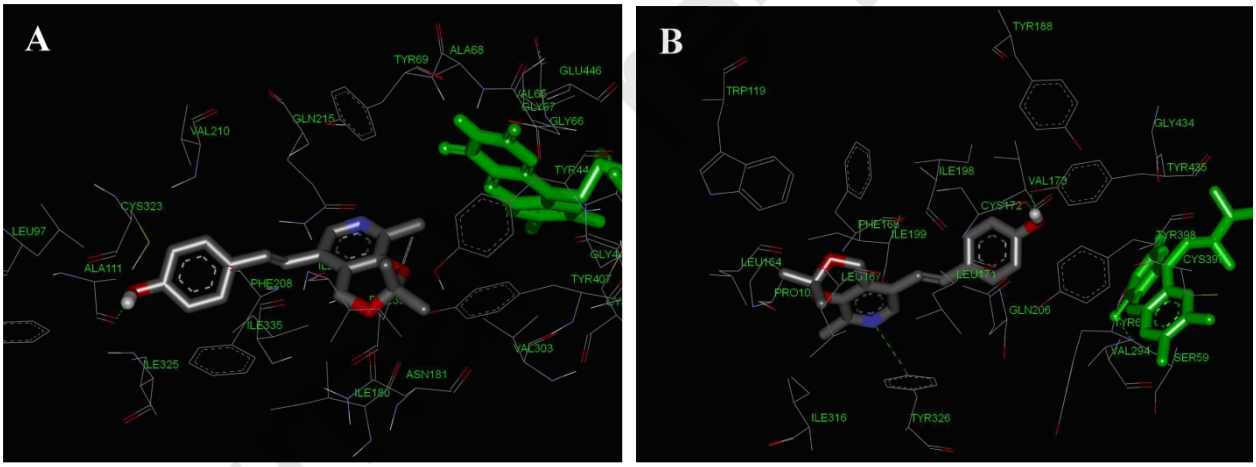

Figure 4 Docking models of the representative compounds with MAO-A (PDB code: *2Z5X*) and -B (PDB code: *2V60*). (A) **12a**-MAO-A complex. (B) **12a**-MAO-B complex. Compound (colored by atom type) interacting with residues in the binding site of MAO-A and -B, highlighting the protein residues that participate in the main interactions with the inhibitors.

Table 2 The binding energies of compound **12a**, **12g**, **12l** with MAO-A and MAO-B.

Comp.[a]	Estimated binding energies (kcal/mol)[b]	
	MAO-A	MAO-B
12a	-9.44	-11.65
12g	-7.69	-12.22
12l	-4.09	-12.86

[a] Representative compounds docked with MAOs based on the X-ray crystal structures of human MAO-A (PDB code: *2Z5X*) and MAO-B (PDB code: *2V60*). [b] The data got from AutoDock 4.2 package.

2.2.4. Antioxidant activity

The antioxidant activities of the pyridoxine-resveratrol hybrids were evaluated by following the oxygen radical absorbance capacity assay that uses fluorescein (ORAC-FL) [37]. The results were displayed as Trolox (a water-soluble vitamin E analogue, which was used as a standard) equivalent. As shown in **Table 1**, the selected representative compounds all showed strong antioxidant activities, and the antioxidant capacity index was between 1.98 and 2.89 Trolox equivalents. Compound **12a** showed the most potent antioxidant activities with an ORAC-FL value of 2.89 Trolox equivalents. And the representative compounds **12g**, **12l** had almost the same antioxidant capacity (2.53 and 2.43 Trolox equivalents). In addition, the length of chain amine groups may influence the antioxidant activities. **12e** bearing dimethylamino group showed more potent radical scavenge ability than **12f** bearing diethylamino group, indicating the increase of carbon chain length may not be beneficial for the antioxidant activities. The antioxidant activities of all tested representative compounds which contained different substituted amines showed no obvious difference.

2.2.5. In vitro blood-brain barrier permeation assay

For a successful CNS drug, it must have the ability to cross the blood brain barrier (BBB) easily and penetrate into the brain. To predict the brain penetration of the targeted compounds, **12a**, **12g** and **12l** were selected to be representative compounds. At the same time, the parallel artificial membrane permeation assay of the blood-brain barrier (PAMPA-BBB) was performed as reported [38]. First, we compared the permeability of 11 commercial drugs with reported values to validate the assay. A plot of experimental data versus reported values gave a good linear correlation, P_e (exp.) = 0.9163 × P_e (bibl.) − 0.2247 (r^2 = 0.9558). From this equation and in view of the limit established by Di *et al.* for BBB permeation, it can be concluded that compounds with P_e values overtopping 3.44 × 11^{-6} cm/s could cross the blood-brain barrier. The results in **Table 3** demonstrated that **12a**, **12g** and **12l** could penetrate into the CNS with good BBB permeability. It reflected that these representative compounds might become potential drugs of the central nervous system diseases. And the results were consistent with our design strategy.

Table 3 Permeability results P_e (× 10^{-6} cm/s) from the PAMPA-BBB assay for **12a**, **12g** and **12l** with the predicted penetration into the CNS.

Compounds[a]	P_e (× 11^{-6} cm/s)[b]	Prediction
12a	6.15 ± 0.35	CNS +
12g	7.12 ± 0.41	CNS +
12l	6.69 ± 0.77	CNS +

[a] Representative compounds were dissolved in DMSO at 5 mg/mL, and diluted with PBS/EtOH (70:30). The final concentration of the compounds was 100 μg/mL.

[b] Data are the mean ± SD of three independent experiments.

2.2.6 Neuroprotective effect on H_2O_2-induced PC-12 cell injury

To examine the cytotoxicity of the representative compounds **12a**, **12g** and **12l**, PC-12 cells were incubated with **12a**, **12g**, **12l** at three different concentrations (10, 50 and 100 μM), and the cell viability was tested using the MTT assay [39]. The active mitochondria of living cells can cleave MTT to produce formazan, the amount of formazan was a direct reflection of the living cell number. As shown in **Fig.5**, compounds **12a**, **12g** and **12l** showed no influence on the cell viability at the concentration of 10 μM. However, when the concentration was increased to 50 μM, **12a**, **12g** and **12l** induced a decrease of cell viability (83%, 85% and 82% of the control value). These results revealed that these representative compounds had a wide therapeutic safety range up to 10 μM and showed cytotoxicity at 50 μM. For the further neuroprotective effect evaluation, as shown in **Fig.6**, cell viability remarkably decreased to 58% of the control value after exposure PC-12 cells to 100 μM H_2O_2, suggesting that PC-12 cells were highly sensitive to H_2O_2. However, when the cells were preincubated with compounds **12a**, **12g** and **12l** (1 μM, 10 μM, 50 μM), H_2O_2-induced cell toxicity significantly attenuated. The three compounds at 10 μM resulted in about 20% recovery from H_2O_2-induced cell injury without cytotoxicity and showed concentration dependency. And their neuroprotective effect at 10 μM can be similar to or better than the neuroprotective effect of Trolox (100 μM). The results showed that these representative compounds had great neuroprotective effect on H_2O_2-induced PC-12 cell injury. In addition, the reduced cell viability at 50 μM of **12a**, **12g**, **12l** might be the comprehensive impact result of the neuroprotective effect and cytotoxicity.

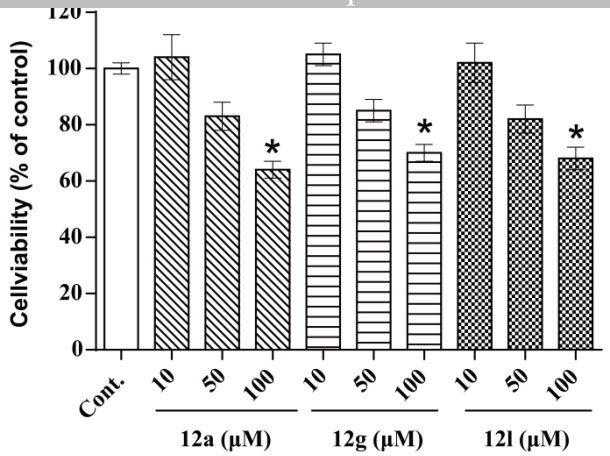

Figure 5 Cell viability was assessed by measuring the MTT reduction. Three independent experiments were carried out in triplicate. Data were expressed as mean ± SD and percentage of the Cont. value. * $p < 0.05$ *vs.* Cont. group.

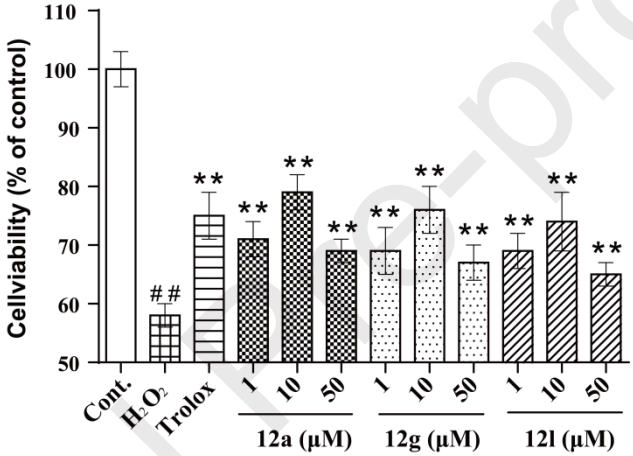

Figure 6 Neuroprotective effects of **12a**, **12g** and **12l** toward PC-12 cells. Cell viability was assessed by measuring the MTT reduction. Three independent experiments were carried out in triplicate. Data were expressed as mean ± SD and percentage of the control value. ## $p < 0.01$ *vs* control; ** $p < 0.01$ *vs* model group (exposure PC-12 cells to H_2O_2 and without adding any compound).

3. Conclusion

A series of pyridoxine-resveratrol hybrids were designed, synthesized and evaluated as MAO-B inhibitors for the treatment of PD. *In vitro* assays demonstrated that most of them exerted high selective and reversibility inhibitory potency on MAO-B, some of them also performed good antioxidant activities. Among all the target compounds, **12a**, **12g** and **12l** exhibited significant antioxidant activities and excellent inhibitory potency for MAO-B with the IC_{50} values of 0.01 μM, 0.01 μM and 0.02 μM. In addition, these three representative compounds also showed high BBB permeability. Furthermore, neuroprotective effect of the three compounds on H_2O_2-induced PC-12

cell injury showed that they had a wide therapeutic safety range and great neuroprotective effects. These properties highlighted that compounds **12a**, **12g** and **12l** might become promising and excellent MAO-B inhibitors for the treatment of PD.

4. Experimental section

4.1. Chemistry

Unless otherwise noted, all of the materials and reagents were obtained commercially and used without further purification. All the air sensitive reactions were performed under argon, and all the reactions were monitored by thin-layer chromatography (TLC) on silica gel GF254 plates from Qingdao Haiyang Chemical Co. Ltd. (China), and spots were visualized in an iodine chamber or with an UV light (254 nm). Column chromatography was performed on silica gel (230-400 mesh) purchased from Qingdao Haiyang Chemical Co. Ltd (China). Melting points (uncorrected) were recorded on YRT-3 melting-point apparatus (China). ^{1}H NMR and ^{13}C NMR spectra were recorded using TMS (Tetramethylsilicane) as the internal standard at the temperature 25 °C in $CDCl_3$ with a Varian INOVA 400 NMR spectrometer. Chemical shifts are reported in parts per millions (ppm) relative to TMS and the coupling constants in Hz. Mass spectra were recorded on Agilent-6211 TOF LC-MS Spectrometer.

*4.1.1 4-(methoxymethoxy)benzaldehyde (**2**)*

p-Hydroxybenzaldehyde (**1**, 1.00 g, 8.19 mmol), acetone (9 mL) and anhydrous K_2CO_3 (2.26 g, 16.38 mmol) were added to the reaction bottle. And the mixture was stirred at room temperature for 15 min. Then a solution of chlormethyl methyl ether (0.75mL, 9.83 mmol) in acetone (3.5 mL) was added dropwise. The mixture was refluxed for 4 h under argon. After the reaction was completed, acetone was removed under reduced pressure. The residue was diluted with water (50 mL), and extracted with ethyl acetate (25 mL × 3). The combined organic phases were washed with brine, dried over anhydrous Na_2SO_4, filtered, and concentrated under reduced pressure to obtain compound **2** as colorless oil, which was used without further purification.

*4.1.2 4-(methyl(prop-2-yn-1-yl)amino)benzaldehyde (**2-1g**)*

Aniline (**3**, 0.30 mL, 3.36 mmol), DMF (2.5 mL) and anhydrous K_2CO_3 (697 mg, 5.04 mmol) were added to the reaction bottle. And the mixture was stirred at room temperature under argon for 30 min. Then a solution of propargyl bromide (0.40 mL, 5.04 mmol) in DMF (1.5 mL) was slowly dropped into the mixture. The mixture was continued to react at room temperature for 5 h under argon. Then the mixture was poured into ice water and extracted with ethyl acetate (15 mL × 3). The

combined organic phases were washed with brine, dried over anhydrous Na_2SO_4, filtered, and concentrated under reduced pressure to afford crude product. After purification by thin-layer chromatography on silica gel, the pure compound **4** (231 mg, 52.3%) was obtained as a yellow oil.

The prepared propargylaniline (**4**, 228 mg, 1.74 mmol), anhydrous K_2CO_3 (360 mg, 2.61 mmol) and dry acetone (15 mL) were added to the reaction bottle. The mixture was stirred at room temperature for 30 min, and dimethyl sulfate (0.20 mL, 2.10 mmol) was dropped into the mixture. After the addition was completed, the mixture was refluxed for 4 h. Then the mixture was poured into ice water and extracted with ethyl acetate (15 mL × 3). The combined organic phases were washed with brine, dried over anhydrous Na_2SO_4, filtered, and concentrated under reduced pressure to obtain compound **5** (230 mg) as a yellow oil, which was used without further purification.

The obtained methylpropargylaniline (**5**, 153 mg, 1.16 mmol), phosphorus oxychloride (0.12 mL, 1.16 mmol) and DMF (5.0 mL) were added to the dry reaction bottle. The mixture was stirred at 30 ^oC for 3 h under argon. Then the reaction mixture was basified with saturated aqueous solution of Na2CO3 and extracted with ethyl acetate (15 mL × 3). The combined organic phases were washed with brine, dried over anhydrous Na_2SO_4, filtered, and concentrated under reduced pressure to get crude product **2-1g**. Without purification, **2-1g** was directly used for further reaction.

*4.1.3 4-(di(prop-2-yn-1-yl)amino)benzaldehyde (**2-1h**)*

In the preparation of propargylidene aniline, the ratio of aniline to propargylidene bromide was 1:2.5, and the other reaction conditions were the same as that of propargylidene aniline. The obtained *N*,*N*-di(prop-2-yn-1-yl)aniline (**6**, 51 mg, 0.30 mmol), phosphorus oxychloride (0.03 mL, 0.30 mmol) and DMF (2.5 mL) were added to a dry reaction bottle and reacted at 30 ^oC for 3 h under argon. Then the mixture was basified with saturated aqueous solution of Na_2CO_3 and extracted with ethyl acetate (15 mL × 3). The combined organic phases were washed with the brine, dried over anhydrous Na_2SO_4, filtered, and concentrated under reduced pressure to obtain crude product **2-1h**, which can be directly used for further reaction without purification.

*4.1.4. General procedure for the synthesis of **2-1i-m***

p-Fluorobenzaldehyde (0.86 mL, 8.06 mmol), corresponding secondary amines (9.67 mmol), anhydrous K_2CO_3 (2.23 g, 16.12 mmol) and DMF (10 mL) were added to the reaction bottle. The mixture was stirred at 100 ^oC for 4-6 h under argon. After the reaction was completed, the mixture was poured into ice water and the corresponding solid was precipitated. The solid was filtered and

washed with ice water. And then the solid was collected and dried at room temperature to obtain the corresponding substituted benzaldehydes (**2-1i-m**).

4.1.4.1 Preparation of compound 2i-m by general procedure

4-(pyrrolidin-1-yl)benzaldehyde (**2-1i**)

A light yellow solid, 68.0% yield; mp: 77.4-79.8 °C (lit.78-80 °C) [40].

4-(piperidin-1-yl)benzaldehyde (**2-1j**)

A light yellow solid, 64.0% yield; mp: 61.7-63.9 °C (lit.65-66 °C) [41].

4-morpholinobenzaldehyde (**2-1k**)

A white solid, 72.0% yield; mp: 62,8-64,4 °C (lit.62-63 °C) [40].

4-(4-methylpiperazin-1-yl)benzaldehyde (**2-1l**)

A light yellow solid, 81.0% yield; mp: 58.0-60.7 °C (lit.58-60 °C) [42].

4-(4-ethylpiperazin-1-yl)benzaldehyde (**2-1m**)

A yellow oil, 61.3% yield.

*4.1.5 Synthesis of (2,2,8-trimethyl-4H-[1,3]dioxino[4,5-c]pyridin-5-yl)methanol (**9**)*

To a mixture of pyridoxine hydrochloride (**8**, 5.00 g, 24.31 mmol) in acetone (100 mL) was added concentrated sulfuric acid (10 mL) dropwise at room temperature. The mixture was stirred at room temperature for 24 h. Then the mixture was basified with saturated aqueous solution of Na_2CO_3 and the organic solvent was evaporated under reduced pressure. The residue was dissolved in dichloromethane (40 mL × 3), then the mixture was washed with water and brine, dried over anhydrous Na_2SO_4, filtered and concentrated under reduced pressure to provide crude product. The cude product was recrystallized from ethyl acetate to give compound **9** (3.12 g, 61.3%) as a white crystal. mp: 108-109 °C (lit.113-115 °C) [43].

*4.1.6. Synthesis of 5-(chloromethyl)-2,2,8-trimethyl-4H-[1,3]dioxino [4,5-c]pyridine (**10**)*

Compound **9** (3.00 g, 14.39 mmol) was dissolved in toluene (50 mL) and thionyl chloride (2.20 mL, 30.24 mmol) in toluene (10 mL) was added dropwise. The mixture was refluxed for 40 min. Then the mixture was directly filtered and washed by toluene to afford a brown-gray solid compound **10** (2.75 g, yield 84.0%). mp: 181-184 °C (lit.185-187 °C) [44].

*4.1.7 Synthesis of diethyl(2,2,8-trimethyl-4H-[1,3]dioxino[4,5-c]pyridin-5-yl)methyl)phosphonate (**11**)*

A mixture of compound **10** (2.47 g, 9.35 mmol) and $P(OEt)_3$ (18 mL) was refluxed for 4 h under

argon. Then the mixture was purified by column chromatography on silica gel using a mixture of petroleum ether/ethyl acetate (1:1) as eluent to give intermediate **11** (2.83 g, yield 92.0%) as a light yellow oil.

*4.1.8 Synthesis of (E)-5-(4-(methoxymethoxy)styryl)-2,2,8-trimethyl-4H-[1,3]dioxino[4,5-c]pyridine (**14**)*

To a mixture of NaH (146 mg, 6.08 mmol) in THF (2 mL) was added a solution of intermediate **11** (500 mg, 1.52 mmol) in THF (4 mL) at 0 °C and the mixture was stirred for 40 min under argon. Then a solution of 4-(methoxymethoxy)benzaldehyde (253 mg, 1.52 mmol) in THF (1 mL) was added dropwise, and the mixture was stirred for another 5 h under argon. The mixture was quenched with 3 mol/L HCl and basified with saturated aqueous solution of Na_2CO_3. Then the mixture was extracted with ethyl acetate (15 mL × 3). The combined organic phases were washed with brine, dried over anhydrous Na_2SO_4, filtered and concentrated under reduced pressure to provide crude product. The crude product was purified on silica gel chromatography using mixtures of petroleum ether/ethyl acetate (2:1) as eluent to afford compound **14** (292 mg, yield 56.3%) as a colorless oil.

*4.1.9 Synthesis of (E)-4-(hydroxymethyl)-5-(4-hydroxystyryl)-2-methylpyridin-3-ol (**15**)*

The intermediate **14** (509 mg, 1.49 mmol) was dissolved in THF (8 mL), and an aqueous solution of HCl (10%, 8 mL) was added. The mixture was refluxed for 3 h under argon. Then THF was removed under reduced pressure. The residue was basified with saturated aqueous solution of Na_2CO_3 and extracted with ethyl acetate (20 mL × 3). The combined organic phases were washed with brine, dried over anhydrous Na_2SO_4, filtered and concentrated under reduced pressure to provide crude product. The crude product was purified on silica chromatography using mixtures of petroleum ether/ethyl acetate (2:1) as eluent to afford **15** (337 mg, yield 87.8%) as a light yellow oil.

*4.1.10 Synthesis of (E)-4-(2-(2,2,8-trimethyl-4H-[1,3]dioxino[4,5-c]pyridin-5-yl)vinyl)phenol (**12a**)*

The intermediate **15** (49 mg, 0.19 mmol) was dissolved in acetone (1 mL) and concentrated sulfuric acid (0.1 mL) was added dropwise at room temperature. The mixture was stirred at room temperature for 3 h under argon. Then the mixture was basified with saturated aqueous solution of Na_2CO_3 and extracted with ethyl acetate (15 mL × 3). The combined organic phases were washed with brine, dried over anhydrous Na_2SO_4, filtered and concentrated under reduced pressure to provide crude product. The crude product was purified on silica gel chromatography using mixtures of petroleum ether/ethyl acetate (3:2) as eluent to afford **12a** as light yellow oil. yield 29.4%; ^{1}H

NMR (400 MHz, $CDCl_3$) δ 8.24 (s, 1H), 7.37 (d, J = 8.4 Hz, 2H), 6.97 (d, J = 16.0 Hz, 1H), 6.89 (d, J = 8.4 Hz, 2H), 6.66 (d, J = 16.0 Hz, 1H), 4.92 (s, 2H), 2.45 (s, 3H), 1.59 (s, 6H); MS (ESI) m/z: 298.0 $[M+H]^+$.

*4.1.11 General procedure for the synthesis of **12b-m***

To a mixture of NaH (146 mg, 6.08 mmol) in THF (2 mL) was added a solution of intermediate **11** (500 mg, 1.52 mmol) in THF (4 mL) at 0 °C, and the mixture was stirred for 40 min under argon. And a solution of corresponding substituted benzaldehydes (**2-1b-m**, 1.52 mmol) in THF (1 mL) was added dropwise. Then the mixture was stirred for another 4-7 h under argon. After the reaction was completed, the mixture was quenched with 3 mol/L HCl and basified with saturated aqueous solution of Na_2CO_3. Then the mixture was extracted with ethyl acetate (15 mL × 3) and the combined organic phases were washed with brine, dried over anhydrous Na_2SO_4, filtered and concentrated under reduced pressure to provide crude product, the crude product was purified on silica chromatography to afford corresponding target compounds **12b-m**.

*4.1.11.1 (E)-5-(4-chlorostyryl)-2,2,8-trimethyl-4H-[1,3]dioxino[4,5-c]pyridine (**12b**)*

Compound **12b** was synthesized from **11** and **2-1b** according to the general procedure. After purification by chromatography on silica gel using petroleum ether/ethyl acetate (5:2) as eluent, the pure product **12b** was obtained as a light yellow solid, 55.6% yield; mp 136.3-138.2 °C; ^{1}H NMR (400 MHz, $CDCl_3$) δ 8.26 (s, 1H), 7.42 (d, J = 8.4 Hz, 2H), 7.34 (d, J = 8.4 Hz, 2H), 6.97 (d, J = 16.0 Hz, 1H), 6.82 (d, J = 16.0 Hz, 1H), 4.91 (s, 2H), 2.43 (s, 3H), 1.57 (s, 6H); ^{13}C NMR (100 MHz, $CDCl_3$) δ 146.8, 145.6, 137.4, 135.1, 133.8, 130.7, 128.9 (2C), 127.8 (2C), 126.9, 123.6, 121.6, 99.5, 59.1, 24.6 (2C), 18.5.

*4.1.11.2 (E)-2,2,8-trimethyl-5-(4-methylstyryl)-4H-[1,3]dioxino[4,5-c]pyridine (**12c**)*

Compound **12c** was synthesized from **11** and **2-1c** according to the general procedure. After purification by chromatography on silica gel using petroleum ether/ethyl acetate (5:2) as eluent, the pure product **12c** was obtained as a colorless oil, 49.6% yield; ^{1}H NMR (400 MHz, $CDCl_3$) δ 8.27 (s, 1H,), 7.39 (d, J = 8.0 Hz, 2H), 7.18 (d, J = 8.0 Hz, 2H), 6.99 (d, J = 16.0, 1H), 6.80 (d, J = 16.0 Hz, 1H), 4.91 (s, 2H), 2.42 (s, 3H), 2.37(s, 3H), 1.57 (s, 6H); ^{13}C NMR (100 MHz, $CDCl_3$) δ 146.3, 145.5, 138.2, 137.3, 133.9, 132.0, 129.4(2C), 127.4, 126.5(2C), 123.5, 120.0, 99.4, 59.2, 24.6(2C), 21.2, 18.4.

*4.1.11.3.(E)-5-(4-methoxystyryl)-2,2,8-trimethyl-4H-[1,3]dioxino[4,5-c]pyridine (**12d**)*

Compound **12d** was synthesized from **11** and **2-1d** according to the general procedure. After purification by chromatography on silica gel using petroleum ether/ethyl acetate (3:1) as eluent, the pure product **12d** was obtained as a yellow oil, 31.7% yield; ^{1}H NMR (400 MHz, $CDCl_3$) δ 8.26 (s, 1H,), 7.43 (d, J = 8.0 Hz, 2H), 6.97 (d, J = 16.0 Hz, 1H), 6.91 (d, J = 8.0 Hz, 2H), 6.70 (d, J = 16.0 Hz, 1H), 4.91 (s, 2H), 3.83 (s, 3H), 2.42 (s, 3H), 1.57 (s, 6H); ^{13}C NMR (100 MHz, $CDCl_3$) δ 159.7, 146.0, 145.5, 137.2, 131.6, 129.4, 127.9 (2C), 127.5, 123.4, 128.7, 124.1 (2C), 99.4, 59.1, 55.2, 24.6 (2C), 18.4.

*4.1.11.4 (E)-N,N-dimethyl-4-(2-(2,2,8-trimethyl-4H-[1,3]dioxino[4,5-c]pyridin-5-yl)vinyl)aniline (**12e**)*

Compound **12e** was synthesized from **11** and **2-1e** according to the general procedure. After purification by chromatography on silica gel using petroleum ether/ethyl acetate (5:2) as eluent, the pure product **12e** was obtained as a light yellow oil, 45.3% yield; ^{1}H NMR (400 MHz, $CDCl_3$) δ 8.26 (s, 1H), 7.39 (d, J = 9.2 Hz, 2H), 6.96 (d, J = 16.0 Hz, 1H), 6.71(d, J = 9.2 Hz, 2H), 6.62 (d, J = 16.0 Hz, 1H), 4.91 (s, 2H), 3.00 (s, 6H), 2.42 (s, 3H), 1.57 (s, 6H); ^{13}C NMR (100 MHz, $CDCl_3$) δ 150.4, 145.3, 136.9, 132.3, 129.8, 128.1, 127.8 (2C), 124.9, 123.3, 126.2, 122.2 (2C), 99.4, 59.3, 40.3 (2C), 24.7 (2C), 18.3; MS (ESI) m/z: 325.2 $[M+H]^+$.

*4.1.11.5 (E)-N,N-diethyl-4-(2-(2,2,8-trimethyl-4H-[1,3]dioxino[4,5-c]pyridin-5-yl)vinyl)aniline (**12f**)*

Compound **12f** was synthesized from **11** and **2-1f** according to the general procedure. After purification by chromatography on silica gel using petroleum ether/ethyl acetate (3:2) as eluent, the pure product **12f** was obtained as a light yellow oil, 53.2% yield; ^{1}H NMR (400 MHz, $CDCl_3$) δ 8.25 (s, 1H), 7.36 (d, J = 8.8 Hz, 2H), 6.94 (d, J = 16.0 Hz, 1H), 6.66 (d, J = 8.8 Hz, 2H), 6.58 (d, J = 16.0 Hz, 1H), 4.90 (s, 2H), 3.39 (q, J = 7.2 Hz, 4H), 2.41 (s, 3H), 1.57 (s, 6H), 1.18 (t, J = 7.2 Hz, 6H); ^{13}C NMR (100 MHz, $CDCl_3$) δ 147.8, 145.6, 145.2, 136.9, 132.3, 128.3, 128.1 (2C), 123.9, 123.2, 125.6, 121.5 (2C), 99.3, 59.3, 44.4 (2C), 24.7 (2C), 18.4, 12.6 (2C); MS (ESI) m/z: 353.0 $[M+H]^+$.

*4.1.11.6 (E)-N-methyl-N-(prop-2-yn-1-yl)-4-(2-(2,2,8-trimethyl-4H-[1,3]dioxino[4,5-c]pyridin-5-yl) vinyl)aniline (**12g**)*

Compound **12g** was synthesized from **11** and **2-1g** according to the general procedure After purification by chromatography on silica gel using petroleum ether/ethyl acetate (3:1) as eluent, the pure product **12g** was obtained as a yellow oil, 36.9% yield; ^{1}H NMR (400 MHz, $CDCl_3$) δ 8.26 (s, 1H,), 7.42 (d, J=8.4 Hz, 2H), 6.96 (d, J=16.0 Hz, 1H), 6.84 (d, J=8.4 Hz, 2H), 6.66 (d, J=16.0 Hz,

1H), 4.91 (s, 2H), 4.09 (d, *J*=2.0 Hz, 2H), 3.02(s, 3H), 2.42 (s, 3H), 2.20 (t, *J*=2.0 Hz, 1H), 1.57 (s, 6H); ^{13}C NMR (100 MHz, $CDCl_3$) δ 148.6, 146.1, 142.2, 137.8, 132.0, 129.8, 127.8 (2C), 126.7, 123.6, 127.3, 123.9 (2C), 99.4, 78.9, 72.1, 59.3, 42.2, 38.5, 24.7 (2C), 18.4; MS (ESI) m/z: 349.1 $[M+H]^+$.

*4.1.11.7 (E)-N,N-di(prop-2-yn-1-yl)-4-(2-(2,2,8-trimethyl-4H-[1,3]dioxino[4,5-c]pyridin-5-yl)vinyl) aniline (**12h**)*

Compound **12h** was synthesized from **11** and **2-1h** according to the general procedure. After purification by chromatography on silica gel using petroleum ether/ethyl acetate (3:1) as eluent, the pure product **12h** was obtained as a light yellow oil, 40.2% yield; ^{1}H NMR (400 MHz, $CDCl_3$) δ 8.28 (s, 1H), 7.44 (d, *J* = 8.8 Hz, 2H), 7.01 (d, *J* = 16.0 Hz, 1H), 6.95 (d, *J* = 8.8 Hz, 2H), 6.66 (d, *J* = 16.0 Hz, 1H), 4.94 (s, 2H), 4.17 (d, *J* = 2.0 Hz, 4H), 2.50 (s, 3H), 2.77 (t, *J* = 2.0 Hz, 2H), 1.59 (s, 6H); ^{13}C NMR (100 MHz, $CDCl_3$) δ 147.8, 146.3, 144.3, 134.5, 133.1, 128.8, 127.9 (2C), 127.4, 125.4, 126.6, 125.1 (2C), 110.0, 78.8 (2C), 72.8 (2C), 59.2, 40.3 (2C), 24.6 (2C), 17.1; MS (ESI) m/z: 373.2 $[M+H]^+$.

*4.1.11.8 (E)-2,2,8-trimethyl-5-(4-(pyrrolidin-1-yl)styryl)-4H-[1,3]dioxino[4,5-c]pyridine (**12i**)*

Compound **12i** was synthesized from **11** and **2-1i** according to the general procedure After purification by chromatography on silica gel using petroleum ether/ethyl acetate (1:1) as eluent, the pure product **12i** was obtained as a yellow oil, 44.6% yield; ^{1}H NMR (400 MHz, $CDCl_3$) δ 8.26 (s, 1H), 7.38 (d, *J* = 8.4 Hz, 2H), 6.96 (d, *J* = 16.0 Hz, 1H), 6.58 (d, *J* = 8.4 Hz, 2H), 6.55 (d, *J* = 16 Hz, 1H), 4.91 (s, 2H), 4.33 (s, 4H), 2.42 (s, 3H), 2.02 (s, 4H), 1.57 (s, 6H); ^{13}C NMR (100 MHz, $CDCl_3$) δ 148.0, 146.4, 145.0, 136.7, 132.7, 128.4, 128.0 (2C), 124.0, 125.3, 121.7 (2C), 99.4, 59.3, 47.6 (2C), 25.4 (2C), 24.7 (2C), 18.2; MS (ESI) m/z: 351.2 $[M+H]^+$.

*4.1.11.9 (E)-2,2,8-trimethyl-5-(4-(piperidin-1-yl)styryl)-4H-[1,3]dioxino[4,5-c]pyridine (**12j**)*

Compound **12j** was synthesized from **11** and **2-1j** according to the general procedure After purification by chromatography on silica gel using petroleum ether/ethyl acetate (7:2) as eluent, the pure product **12j** was obtained as a light yellow oil, 38.5% yield; ^{1}H NMR (400 MHz, $CDCl_3$) δ 8.25 (s, 1H), 7.36 (d, *J* = 8.4 Hz, 2H), 6.94 (d, *J* = 16.0 Hz, 1H), 6.90(d, *J* = 8.4 Hz, 2H), 6.66 (d, *J* = 16.0 Hz, 1H), 4.91 (s, 2H), 3.22 (t, *J* = 5.2 Hz, 4H), 2.42 (s, 3H), 1.71 (t, *J* = 5.2 Hz, 4H), 1.63-1.60 (m, 2H,), 1.57 (s, 6H); ^{13}C NMR (100 MHz, $CDCl_3$) δ 151.8, 145.7, 145.5, 137.1, 132.0, 127.9, 127.6 (2C), 127.1, 123.3, 127.3, 125.8 (2C), 99.4, 59.3, 48.9 (2C), 25.6 (2C), 24.7 (2C), 24.3, 18.4; MS

(ESI) m/z: 365.1 $[M+H]^+$.

*4.1.11.10 (E)-2,2,8-trimethyl-5-(4-morpholinostyryl)-4H-[1,3]dioxino[4,5-c]pyridine (**12k**)*

Compound **12k** was synthesized from **11** and **2-1k** according to the general procedure. After purification by chromatography on silica gel using petroleum ether/ethyl acetate (2:1) as eluent, the pure product **12k** was obtained as a yellow oil, 40.3% yield; ^{1}H NMR (400 MHz, $CDCl_3$) δ 8.26 (s, 1H,), 7.42 (d, J = 8.4 Hz, 2H), 6.96 (d, J = 16.0 Hz, 1H), 6.90(d, J = 8.4 Hz, 2H), 6.69 (d, J = 16.0 Hz, 1H), 4.91 (s, 2H), 3.87 (t, J = 4.4 Hz, 4H), 3.21 (t, J = 4.4 Hz, 4H), 2.42 (s, 3H), 1.57 (s, 6H); ^{13}C NMR (100 MHz, $CDCl_3$) δ 151.1, 145.9, 145.5, 137.2, 131.7, 128.2, 127.7 (2C), 123.3, 128.1, 125.3 (2C), 118.8, 99.4, 66.7 (2C), 59.2, 48.7 (2C), 24.6 (2C), 18.4; MS (ESI) m/z: 367.0 $[M+H]^+$.

*4.1.11.11 (E)-2,2,8-trimethyl-5-(4-(4-methylpiperazin-1-yl)styryl)-4H-[1,3]dioxino[4,5-c]pyridine (**12l**)*

Compound **12l** was synthesized from **11** and **2-1l** according to the general procedure. After purification by chromatography on silica gel using petroleum ether/acetone (2:1) as eluent, the pure product **12l** was obtained as a light yellow oil, 55.7% yield; ^{1}H NMR (400 MHz, $CDCl_3$) δ 8.25 (s, 1H), 7.40 (d, J = 8.8 Hz, 2H), 6.95 (d, J = 16.0 Hz, 1H), 6.91 (d, J = 8.8 Hz, 2H), 6.67 (d, J = 16.0 Hz, 1H), 4.91 (s, CH_2), 3.28 (t, J = 4.8 Hz, 4H), 2.60 (t, J = 4.8 Hz, 4H), 2.41 (s, 3H), 2.37 (s, 3H), 1.57 (s, 6H); ^{13}C NMR (100 MHz, $CDCl_3$) δ 151.0, 145.8, 145.5, 137.2, 131.8, 127.9, 127.7, 127.6 (2C), 123.3, 127.8, 125.5 (2C), 99.3, 59.2, 54.8 (2C), 48.4 (2C), 46.0, 24.6 (2C), 18.4; MS (ESI) m/z: 380.2 $[M+H]^+$.

*4.1.11.12 (E)-5-(4-(4-ethylpiperazin-1-yl)styryl)-2,2,8-trimethyl-4H-[1,3]dioxino[4,5-c]pyridine (**12m**)*

Compound **12m** was synthesized from **11** and **2-1m** according to the general procedure. After purification by chromatography on silica gel using dichloromethane/methanol (30:1) as eluent, the pure product **12m** was obtained as a yellow oil, 24.0% yield; ^{1}H NMR (400 MHz, $CDCl_3$) δ 8.25 (s, 1H), 7.41 (d, J = 8.4 Hz, 2H), 6.95 (d, J = 16.0 Hz, 1H), 6.92 (d, J = 8.4 Hz, 2H), 6.68 (d, J = 16.0 Hz, 1H), 4.91 (s, 2H), 3.31 (t, J = 4.8 Hz, 4H), 2.67 (t, J = 4.8 Hz, 4H), 2.53 (q, J = 7.2 Hz, 2H), 2.41 (s, 3H), 1.57 (s, 6H), 1.17 (t, J=7.2 Hz, 3H); ^{13}C NMR (100 MHz, $CDCl_3$) δ 151.0, 145.8, 145.5, 137.2, 131.8, 127.9, 127.7, 127.6 (2C), 123.3, 127.9, 125.6 (2C), 99.4, 59.2, 52.5 (2C), 52.3, 48.3 (2C), 24.6 (2C), 18.4, 12.7; MS (ESI) m/z: 394.2 $[M+H]^+$.

*4.1.12 General procedure for the synthesis of **13a-b***

13a-b was synthesized from *mata*-substituted benzaldehyde according to the general method in 4.1.11 of this article.

*4.1.12.2 (E)-5-(3-chlorostyryl)-2,2,8-trimethyl-4H-[1,3]dioxino[4,5-c]pyridine (**13a**)*

Compound **13a** was synthesized from **11** and **2-2a** according to the general procedure. After purification by chromatography on silica gel using petroleum ether/ethyl acetate (3:1) as eluent, the pure product **13a** was obtained as a yellow solid, 61.3% yield; mp: 129.8-131.3 ^{o}C; ^{1}H NMR (400 MHz, $CDCl_3$) δ 8.26 (s, 1H), 7.44 (s, 1H), 7.36-7.25 (m, 3H), 6.95 (d, J = 16.0 Hz, 1H), 6.86 (d, J = 16.0 Hz, 1H), 4.92 (s, 2H), 2.43 (s, 3H), 1.57 (s, 6H); ^{13}C NMR (100 MHz, $CDCl_3$) δ 147.0, 145.6, 138.5, 137.4, 134.6, 130.5, 129.9, 128.0, 126.7, 126.3, 124.9, 123.7, 122.4, 99.5, 59.0, 24.6 (2C), 18.5.

*4.1.12.3 (E)-5-(3-methoxystyryl)-2,2,8-trimethyl-4H-[1,3]dioxino[4,5-c]pyridine (**13b**)*

Compound **13b** was synthesized from **11** and **2-2b** according to the general procedure. After purification by chromatography on silica gel using petroleum ether/ethyl acetate (3:1) as eluent, the pure product **13b** was obtained as a light yellow oil, 38.0% yield; ^{1}H NMR (400 MHz, $CDCl_3$) δ 8.27 (s, 1H), 7.28 (t, J = 8.0 Hz, 1H), 7.09 (d, J = 8.0 Hz, 1H), 7.01 (s, 1H), 6.98 (d, J = 16.0 Hz, 1H), 6.85 (d, J = 8.0 Hz, 1H), 6.84 (d, J = 16.0 Hz, 1H), 4.91 (s, 2H), 3.84 (s, 3H), 2.43 (s, 3H), 1.57 (s, 6H); ^{13}C NMR (100 MHz, $CDCl_3$) δ 159.8, 146.6, 145.5, 138.1, 137.4, 132.0, 129.7, 127.1, 123.6, 121.3, 129.2, 123.7, 122.0, 99.4, 59.1, 55.2, 24.6 (2C), 18.4.

4.2. Biological evaluation

4.2.1. In vitro inhibition of MAO activity

To further study the biological profile of the target compounds, the inhibitory activity against MAO-A and MAO-B was determined [45]. MAO-A and -B were obtained from commercial sources (Sigma Co.), pre-aliquoted and stored at -80 °C. The target compounds were dissolved in DMSO (2.5 mL) and diluted with potassium phosphate buffer (100 mM, pH = 7.40, containing KCl 20.2 mM) before use. The enzymatic reactions were conducted in potassium phosphate buffer (pH = 7.4, made isotonic with KCl) to a final volume of 500 μL and contained kynuramine, various concentrations of the test compounds and 4% DMSO as cosolvent. The addition of MAO-A or -B (7.5 μg/mL) is a trigger of the reaction, and then the mixture was incubated for 30 min at 37 °C. The reactions were ended by the addition of 400 μL NaOH (2 mol/L) and 1000 μL water and then centrifuged at 16000 g for 10 min. The rates of MAO catalysis can be conveniently determined by

measuring the formation of 4-hydroxyquinoline via fluorescence spectrophotometry at excitation and emission wavelengths of 310 nm and 400 nm, respectively. Samples containing 4-hydroxyquinoline (0.047-1.56 μM) dissolved in 500 μL potassium phosphate buffer were prepared to give a linear calibration curve. IC_{50} values were estimated from sigmoidal dose-response curves (graphs of the initial rate of kynuramine oxidation versus the logarithm of inhibitor concentration) and were determined in triplicate and are expressed as mean ± standard deviation (SD). Each measurement was run in triplicate and each reaction was repeated for at least three times.

4.2.2. Reversibility study of hMAO-B inhibition

The reversibility of the MAO-B inhibition by **12a**, **12g**, **12l** was investigated by dialysis [34] employing dialysis bag (Baoke Scientific, USA) with a molecular weight cut-off of 10000, a flattening width of 24 mm (0.45 mL/cm) and a length of about 8-10 cm. MAO-B (0.03 mg/mL) and **12a**, **12g**, **12l**, at a concentration equal to 4 × IC_{50}, were preincubated for 30 min at 37 °C. These reactions were conducted in potassium phosphate buffer (100 mM, pH 7.4) containing 5% sucrose and the final volume was 0.6 mL. As negative and positive controls, MAO-B was also preincubated in the absence of inhibitor, presence of a concentration equal to 4 × IC_{50} of the irreversible inhibitor, rasagiline (MAO-B IC_{50} = 0.014 μm) and reversible inhibitor safinamide (MAO-B IC_{50} = 0.039 μm). The reactions were subsequently dialyzed at 4 °C in 200 mL outer buffer (100 mM potassium phosphate, pH 7.4, 5.0% sucrose). The outer buffer was replaced with fresh buffer at 3 h and 7 h after the start of dialysis. After dialysis was started for 24 h, the reactions were diluted twofold with the addition of kynuramine (dissolved in potassium phosphate buffer, 100 mM, pH 7.4, made isotonic with KCl), and the residual MAO-B activities were measured as described above (the part of 4.2.1). The final concentration of kynuramine in these reactions was 50 μM while the final inhibitor concentrations were equal to twofold of their IC_{50} values for the inhibition of MAO-B. For comparison, undialyzed mixtures of MAO-B-**12a**, MAO-B-**12g**, MAO-B-**12l**, MAO-B-rasagiline and MAO-B-safinamide were maintained at 4 °C over the same time period. These reactions were carried out in triplicate and the residual enzyme catalytic rates were expressed as mean ± SD.

4.2.3. Antioxidant activity

The antioxidant activity was determined by an oxygen radical absorbance capacity assay that uses fluorescein (ORAC-FL), based on the method previously described [37]. 2,2′-Azo-bis (amidinopropane)dihydrochloride (AAPH) was purchased from Accela ChemBio Co. Ltd.

6-hydroxy-2,5,7,8-tetramethylchromane-2-carboxyic acid (Trolox) and fluorescein (FL) were purchased from TCI (Shanghai) Development. All the assays were conducted in the wells of a black 96-well plate containing 75 mM phosphate buffer (pH = 7.4), antioxidant (20 μL) and fluorescein (120 μL, 150 nM final concentration). The mixture was incubated for 15 min at 37 °C, and then AAPH solution (60 μL, 12 mM final concentration) was added rapidly by an autosampler. The plate was placed in a Varioskan Flash Multimode Reader (Thermo Scientific) immediately, and the fluorescence recorded every minute for 90 min with excitation at 485 nm and emission at 535 nm. The plate was automatically shaken prior to each reading. Trolox, a vitamin E analogue, was used as standard (1-8 μM, final concentration). A blank (FL + AAPH) using phosphate buffer instead of antioxidant and Trolox calibration were carried out in each assay. The samples were performed at different concentration (1-10 μM). All the reaction mixture was prepared in duplicate, and at least three independent assays were performed for each sample. Antioxidant curves (fluorescence versus time) were normalized to the curve of the blank in the same assay, and then the area under the fluorescence decay curve (AUC) was calculated. The net AUC of a sample was obtained by subtracting the AUC of the blank. ORAC-FL values were expressed as Trolox equivalents by using the standard curve calculated for each sample, where the ORAC-FL value of Trolox was taken as 1.0, indicating the antioxidant potency of the tested compounds.

4.2.4. In vitro blood-brain barrier permeation assay

To evaluate the *in vitro* blood-brain barrier permeation assay, the method described by Di *et al.* was used with some modifications [38]. Commercial drugs were purchased from Sigma and Alfa Aesar. Porcine brain lipid (PBL) was obtained from Avanti Polar Lipids. The donor plate (MATRNPS50) and the acceptor plate (PVDF membrane, pore size is 0.45 μm, MAIPN4550) were both from Millipore. Filter PDVF membrane units (diameter 25 mm, pore size 0.45 μm) from Pall Corporation were used to filter the samples. Test compounds were dissolved in DMSO at 5 mg/mL and diluted 50-fold in PBS/EtOH (70:30) to a final concentration of 100 μg/mL. Then 350 μL of the diluted compound solution (100 μg/mL) were added to the donor wells. The acceptor wells were filled with 200 μL of PBS/EtOH (70:30). The filter membrane was coated with PBL in dodecane (selected empirically as 4 μL volume of 20 μg/mL PBL in dodecane). The acceptor filter plate was carefully put on the donor plate to form a sandwich (consisting of the aqueous donor with test compound on the bottom, lipid membrane in the middle and the aqueous acceptor on the top), which

was left undisturbed for 18 h at 25 °C. After incubation, the donor plate was removed and the concentration of the compounds in the acceptor and donor wells was determined using the Varioskan Flash Multimode Reader (Thermo Scientific). Permeability rates (Pe) was calculated using the following expression: $P_e = -\ln [1 - C_A(t)/C_{equilibrium}]/[A \times (1/V_D + 1/V_A) \times t]$ $C_{equilibrium} = [C_D(t) \times V_D + C_A(t) \times V_A]/(V_D + V_A)$, where A is the filter area, t is the permeation time, V_D is the volume of donor well, V_A is the volume in the acceptor well, $C_A(t)$ is the compound concentration in acceptor well at time t, and $C_D(t)$ is the compound concentration in donor well at time t. Eleven quality control standards of known BBB permeability were used to monitor the consistency of each experiment. Every sample was analyzed at ten wavelengths in four wells and in at least three independent runs. The results were given as the mean ± standard deviation.

4.2.5 Neuroprotective effect on H_2O_2-induced PC-12 cell injury

The neuroprotective effect of the representative compounds on H_2O_2-induced PC-12 cell injury was determined using the classical MTT assay [39]. For the cell viability assay, briefly, PC-12 cells were seeded into 96-well plates at a density of 1×10^5 cells per mL in DMEM medium (GIBCO) supplemented with 10% heat-inactivated bovine calf serum (Hyclone). After incubation overnight, the medium was replaced with fresh DMEM medium without calf serum and phenol red. And tested compounds at various concentrations were added and incubated with the cells for further 2 h. Then, H_2O_2 (100 mM) was added and the cells were further incubated for 24 h. At the end of the assay, the cells were incubated with 0.5 mg/mL 3-(4,5-dimethylthiazol-2-yl)-2,5-diphenyltetrazolium bromide (MTT) for 4 h at 37 ℃. The supernatants were carefully removed, and 150 mL DMSO was added to each well. The absorbance at 570 nm of the formazan was determined using a Varioskan Flash Multimode Reader (Thermo Scientifific). Data were expressed as mean ± SD. To determine the cytotoxicity of the compound, tested compound was incubated with PC-12 cells for 48 h without the addition of H_2O_2, and other procedures were similar to the above mentioned.

4.2.6. Molecular modeling study of MAO

The simulation systems were built based on the X-ray crystal structures of *h*MAO-A (PDB code: 2Z5X) and *h*MAO-B (PDB code: 2V60), both are from the Protein Data Bank. The original ligands and water molecules were removed and hydrogen atoms were added to both proteins and cofactors. Pretreatment of small molecules involved performing charge calculations and setting rotable bonds. Then docking study was performed using the AUTODOCK 4.2. The center of the grid box was

placed at the center of original ligand and the dimensions of the active site box were set at 60 × 60 × 60 Å. Each docked system was executed 100 times of the autodock search by using the Lamarckian genetic algorithm (LGA). Based on the docking results, the root mean square (rms) tolerance of 1.0 was used for clustering analysis, and the lowest energy form of the cluster with the highest filling density was selected for analysis. Graphic processing and visualization were accomplished by Autodock Tools 1.5.6 or Discovery Studio 2.5 software.

Acknowledgments

This work was supported by Sichuan Science and Technology Program (2018SZ0014, 2019YFS0088) and the Fundamental Research Funds for the Central Universities.

Appendix A. Supplementary Material

The supplementary data associated with this article can be found in the online version.

References

[1] P.A. Lewis, J.E. Spillane, Chapter 3 Parkinson's disease, in: P.A. Lewis, J.E. Spillane (Eds.), The molecular and clinical pathology of neurodegenerative disease, Academic Press, 2019, pp. 83-121.

[2] S.G. Reich, J.M. Savitt, Parkinson's disease, Med. Clin. North Am. 103 (2019) 337-350.

[3] M.T. Hayes, Parkinson's disease and Parkinsonism, Am. J. Med. 132 (2019) 802-807.

[4] C. Raza, R. Anjum, N.U.A. Shakeel, Parkinson's disease: mechanisms, translational models and management strategies, Life Sci. 226 (2019) 77-90.

[5] E.R. Dorsey, R. Constantinescu., J.P. Thompson, K.M. Biglan, R.G. Holloway, K. Kieburtz, F.J. Marshall, B.M. Ravina, G. Schifitto, A. Siderowf, C.M. Tanner, Projected number of people with Parkinson disease in the most populous nations, 2005 through 2030, Neurology. 68 (2007) 384-386.

[6] S. Carradori, F. Ortuso, A. Petzer, D. Bagetta, C.D. Monte, D. Secci, D. D. Vita, P. Guglielmi, G. Zengin, A. Aktumsek, S. Alcaro, J.P. Petzer, Design, synthesis and biochemical evaluation of novel multi-target inhibitors as potential anti-Parkinson agents, Eur. J. Med. Chem. 143 (2018) 1543-1552.

[7] W. Dauer, S. Przedborski, Parkinson's disease: mechanisms and models, Neuron. 39 (2003) 889-909.

[8] A. Osterhaus, J. Groen, H. Niesters, M. van de Bildt, B. Martina, L. Vedder, J. Vos, H. van Egmond, B.A. Sidi, M.E.O. Barham, Morbillivirus in monk seal mass mortality, Nature. 388 (1997) 838-839.

[9] M. Hemmati-Dinarvand, S. Saedi, M Valilo, A. Kalantary-Charvadeh, M.A. Sani, R. Kargar, H. Safari, N. Samadi, Oxidative stress and Parkinson's disease: conflict of oxidant-antioxidant systems, Neurosci. Lett. 709 (2019) 134296.

[10] B. Dinda, M. Dinda, G. Kulsi, A. Chakraborty, S. Dinda, Therapeutic potentials of plant iridoids in Alzheimer's and Parkinson's diseases: a review, Eur. J. Med. Chem. 169 (2019) 185-199.

[11] M.B.H. Youdim, Y.S. Bakhle, Monoamine oxidase: isoforms and inhibitors in Parkinson's disease and depressive illness, Br. J. Pharmacol. 147 (2006) 287-296.

[12] D.N. Hauser, T.G. Hastings, Mitochondrial dysfunction and oxidative stress in Parkinson's disease and monogenic parkinsonism, Neurobiol. Dis. 51 (2013) 35-42.

[13] J.S. Fowler, N.D. Volkow, G.J. Wang, J. Logan, N. Pappas, C. Shea, R. Macgregor, Age-related increases in brain Monoamine oxidase B in living healthy human subjects, Neurobiol Aging 18 (1997) 431-435.

[14] S.L. Li, D.Y. Wei, Z. Mao, L.G. Chen, X.L. Yan, Y. Li, S.J. Dong, D.H. Wang, Design, synthesis, immunocytochemistry evaluation, and molecular docking investigation of several 4-aminopyridine derivatives as potential neuroprotective agents for treating Parkinson's disease, Bioorg. Chem. 73 (2017) 63-75.

[15] A. Weissbach, K. Udupa, Z. Ni, C. Gunraj, C. Rinchon, J. Baarbe, A. Fasano, R.P. Munhoz, A. Lang, V. Tadic, N. Brüggemann, A. Münchau, T. Bäumer, R. Chen, Single-pulse subthalamic deep brain stimulation reduces premotor-motor facilitation in Parkinson's disease, Parkinsonism Relat. Disord. 66 (2019) 224-227.

[16] J.M. Ellis, M.J. Fell. Current approaches to the treatment of Parkinson's disease, Bioorg. Med. Chem. Lett. 27 (2017) 4247-4255.

[17] A. AlDakheel, L.V. Kalia, A.E. Lang, Pathogenesis-targeted, disease-modifying therapies in Parkinson disease, Neurotherapeutics 11 (2014) 6-23.

[18] R. Morphy, Z. Rankovic, Designed multiple ligands. an emerging drug discovery paradigm, J.

Med. Chem. 48 (2005) 6523-6543.

[19] A. Cavalli, M.L. Bolognesi, A. Minarini, M. Rosini, V. Tumiatti, M. Recanatini, C. Melchiorre, Multi-target-directed ligands to combat neurodegenerative diseases, J. Med. Chem. 51 (2008) 347-372.

[20] H. Wang, T.Y. Jiang, W. Li, N. Gao, T. Zhang, Resveratrol attenuates oxidative damage through activating mitophagy in an in vitro model of Alzheimer's disease, Toxicol. Lett. 282 (2018) 100-108.

[21] M. Inglés, J. Gambini, M. Graca Miguel, V. Bonet-Costa, K.M. Abdelaziz, M.E. Alami, J. Viña, C. Borrás, PTEN mediates the antioxidant effect of resveratrol at nutritionally relevant concentrations, BioMed Res. Int. 2014 (2014) 1-6.

[22] K. Drygalski, E. Fereniec, K. Koryciński, A. Chomentowski, A. Kiełczewska, C. Odrzygóźdź, B. Modzelewska, Resveratrol and Alzheimer's disease. from molecular pathophysiology to clinical trials, Exp. Gerontol. 113 (2018) 36-47.

[23] D. Clark, U.I. Tuor, R. Thompson, A. Institoris, A. Kulynych, X. Zhang, D.W. Kinniburgh, F. Bari, D.W. Busija, P.A. Barber, Protection against recurrent stroke with resveratrol: endothelial protection, PloS One 7 (2012) e47792.

[24] Y.W. Tang, C.J. Shi, H.L. Yang, P. Cai, Q.H. Liu, X.L. Yang, L.Y. Kong, X.B. Wang, Synthesis and evaluation of isoprenylation-resveratrol dimer derivatives against Alzheimer's disease, Eur. J. Med. Chem. 163 (2019) 307-319.

[25] L. Tang, M.H. Li, P. Cao, F. Wang, W.R. Chang, S. Bach, J. Reinhardt, Y. Ferandin, H. Galons, Y.Q. Wan, N. Gray, L. Meijer, T. Jiang, D.C. Liang, Crystal structure of pyridoxal kinase in complex with roscovitine and derivatives, J. Biol. Chem. 280 (2005) 31220-31229.

[26] N. Yokochi, T. Morita, T. Yagi, Inhibition of diphenolase activity of tyrosinase by vitamin B_6 compounds, J. Agric. Food Chem. 51 (2003) 2733-2736.

[27] A. Hashim, L. Wang, K. Juneja, Y. Ye, Y.F. Zhao, L.J. Ming, Vitamin B6s inhibit oxidative stress caused by Alzheimer's disease-related CuII-β-amyloid complexes-cooperative action of phospho-moiety, Bioorg. Med. Chem. Lett. 21 (2011) 6430-6432.

[28] X. Yang, X.M. Qiang, Y. Li, L. Luo, R. Xu , Y.X.Z. Zheng, Z.C. Cao, Z.H. Tan, Y Deng, Pyridoxine-resveratrol hybrids Mannich base derivatives as novel dual inhibitors of AChE and MAO-B with antioxidant and metal-chelating properties for the treatment of Alzheimer's

disease, Bioorg. Chem. 71 (2017) 305-314.

[29] M. Vedamalai, S.P. Wu, A bodipy-based highly selective fluorescent chemosensor for Hg^{2+} ions and its application in living cell imaging. Eur. J. Org. Chem. 10 (2012), 1158-1163.

[30] H.J. Kumpaty, J.S. Williamson, S. Bhattacharyya, Synthesis of N-methyl secondary amines, Syn. Commun. 33 (2003), 1411-1416.

[31] G. Knobloch, N. Jabari, S. Stadlbauer, H. Schindelin, M. Köhn, A. Gohla, Synthesis of hydrolysis-resistant pyridoxal 5-phosphate analogs and their biochemical and X-ray crystallographic characterization with the pyridoxal phosphatase chronophin, Bioorg. Med. Chem. 23 (2015) 2819-2827.

[32] D. Robakis, S. Fahn, Defining the role of the monoamine oxidase-B inhibitors for Parkinson's disease, CNS Drugs 29 (2015) 433-441.

[33] M. Yamada, H. Yasuhara, Clinical pharmacology of MAO Inhibitors: safety and future, NeuroToxicology 25 (2004) 215-221.

[34] A. Petzer, A. Pienaar, J.P. Petzer, The interactions of caffeine with monoamine oxidase, Life Sci. 93 (2013) 283-287.

[35] C. Binda, F. Hubálek, M. Li, Y. Herzig, J. Sterling, D.E. Edmondson, A. Mattevi, Binding of Rasagiline-related inhibitors to human monoamine oxidases: a kinetic and crystallographic analysis, J. Med. Chem. 48 (2005) 8148-8154.

[36] N. Desideri, A. Bolasco, R. Fioravanti, L.P. Monaco, F. Orallo, M. Yáñez, F. Ortuso, S. Alcaro, Homoisoflavonoids: natural scaffolds with potent and selective monoamine oxidase-B Inhibition properties, J. Med. Chem. 54 (2011) 2155-2164.

[37] L. Huang, C.J. Lu, Y. Sun, F. Mao, Z.H. Luo, T. Su, H.L. Jiang, W.J. Shan, X.S. Li, Multitarget-directed benzylideneindanone derivatives: anti-β-amyloid (Aβ) aggregation, antioxidant, metal chelation, and monoamine oxidase B (MAO-B) Inhibition properties against Alzheimer's disease, J. Med. Chem. 55 (2012) 8483-8492.

[38] L. Di, E.H. Kerns, K. Fan, O.J. McConnell, G.T. Carter, High throughput artifificial membrane permeability assay for blood brain barrier, Eur. J. Med. Chem. 38 (2003) 223-232.

[39] Y. Li, X.M. Qiang, L. Luo, X. Yang, G.Y. Xiao, Q. Liu, J.C. Ai, Z.H. Tan, Y. Deng, Aurone mannich base derivatives as promising multifunctional agents with acetylcholinesterase inhibition, anti-β-amyloid aggragation and neuroprotective properties for the treatment of

Alzheimer's disease, Eur. J. Med. Chem. 126 (2017) 762-775.

[40] P. Magdolen, M. Mečiarová, Š. Toma, Ultrasound effect on the synthesis of 4-alkyl-(aryl)aminobenzaldehydes, Tetrahedron 57 (2001) 4781-4785.

[41] H.A. Abdel-Aziz, B.F. Abdel-Wahab, M.A.M.S. El-Sharief, M.M. Abdulla, Synthesis and anti-arrhythmic activity of some piperidine-based 1,3-thiazole, 1,3,4-thiadiazole, and 1,3-thiazolo-[2,3-c]-1,2,4-triazole derivatives. Monatsh. Chem, 140 (2009) 431-437.

[42] X.L. Liu, M.L. Go, Antiproliferative activity of chalcones with basic functionalities. Bioorg. Med. Chem. 15 (2007) 7021-7034.

[43] D.Y. Yang, Y.N. Shih, H.W. Liu, Chemical synthesis of stereo specifically labeled pyridoxamine 5'-Phosphate, J. Org. Chem. 56 (1991) 2940-2946.

[44] Y.N. Belokon, V.I. Tararoc, V.I. Bakhmutoc, V.M. Belikoc, Biomimetic approach to the design of a pyridoxal enzyme model, 3. Synthesis of 4-formyl-3-hydroxy-5-methacryloylaminomethyl-2-methylpyridine and its 5'-N-methylated analogue, Makromol. Chem. 184 (1983) 1-7.

[45] L.J. Legoabe, A. Petzer, J.P. Petzer, Selected C7-substituted chromone derivatives as monoamine oxidase inhibitors, Bioorg. Chem. 45 (2012) 1-11.

Declaration of interests

☑ The authors declare that they have no known competing financial interests or personal relationships that could have appeared to influence the work reported in this paper.

☐The authors declare the following financial interests/personal relationships which may be considered as potential competing interests:

Graphical abstract

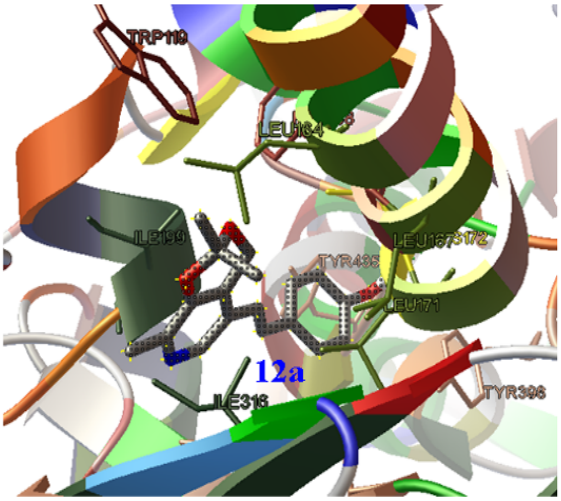

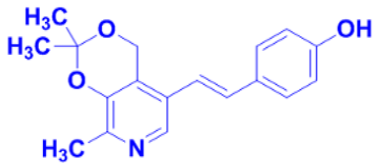

12a

MAO-B inhibition: IC_{50} = 0.01 μM

MAO-A inhibition: 24.1% at 10 μM

Selectivity index > 1000

Reversible inhibition of MAO-B

Antioxidant, ORAC-FL value: 2.89

Neuroprotective on H_2O_2-induced PC-12 cell injury

Good BBB permeability *in vitro*

Highlights

- Novel pyridoxine-resveratrol hybrids were synthesized.
- Most compounds showed selective MAO-B inhibitory and antioxidant activities.
- Compound **12a** and **12l** exhibited tight and reversible connection with MAO-B.
- **12a**, **12g** and **12l** showed good neuroprotective effects.
- These compounds also showed high blood-brain barrier permeability.